

# Metabolic origins of spatial organization in the tumor microenvironment

Garima Lohani, Caroline Muriithi, Brian Spitzer, and Jacquelyn Turcinovic

## Background and Motivation

Cancer tumors are often described as disorganized and chaotic. In contrast, the authors of this article argue that metabolic activity creates spatial gradients similar to those seen in embryonic development, allowing tumor tissues to self-organize and to produce greater efficiency at the level of the entire tumor<sup>1</sup>.

Tumor growth can lead to cells that are too far from a vessel for effective resource supply. The vascular endothelial growth factor VEGF-A (VEGF) is secreted in response to hypoxia and high concentrations of lactate<sup>1</sup>. It dilates microvessels and increases their "leakiness"<sup>2-3</sup>, allowing more resources to flow into the surrounding tissue. VEGF expression is frequently upregulated in cancer cell lines<sup>2,4</sup>, and some cell lines secrete high levels of VEGF constitutively<sup>5</sup>. This strategy has clear advantages for cancer cells, but VEGF secretion also costs resources, and VEGF has powerful angiogenic effects that cause some resources to be redirected away from tumor cells toward the growth of new vessels. Carmona-Fontaine *et al.* hypothesize that if a tumor secretes VEGF only where resources are scarce in a responsive strategy rather than constitutively, it will minimize needless costs and experience faster growth<sup>1</sup>. They present this as an example of spatial self-organization within a cancer tumor that produces greater efficiency.

In their paper, Carmona-Fontaine *et al.* address this hypothesis by constructing a mathematical model of how the balance between costs and benefits of VEGF secretion changes with increasing distance from existing vessels. They also construct an agent-based model to simulate tumor growth when cells follow a responsive or a constitutive strategy. We aimed to reproduce their results in both the theoretical and agent-based models.

## Methods

### Theoretical model

Carmona-Fontaine *et al.* described the derivation of their mathematical model in detail in the paper's Supplementary Information. They assumed a linear or exponential resource density gradient,  $r(x)$  (Eqs. 1-2); a linear cost function for increasing resources via VEGF secretion,  $C(\Delta r)$  (Eq. 3); and a growth rate function dependent on resource density,  $\mu(r)$ , which follows saturating kinetics (Eq. 4). Since a responsive VEGF secretion strategy balances the cost of secreting VEGF with the enhanced growth rate resulting from said secretion, there is an optimal resource density,  $r^{opt}$ , that all cells in the model seek to reach. Since cells may have different starting resource densities, each has a unique change in density,  $\Delta r^{opt}$ , that will increase the starting resource density to the optimal resource density (Eq. 5). Thus, the total profit of investing in increasing the resource density,  $P(x)$ , can be calculated by subtracting the initial growth rate and investment cost from the improved growth rate (Eq. 6). Calculating the optimal profit for each distance from a vessel shows that when the resource density is increased by the  $\Delta r^{opt}$  for each distance, the slope of growth rate function  $\mu(r)$  equals the cost constant (Eq. 7).

Combining equation 7 and equation 5 results in the analytical solution to  $\Delta r^{opt}(x)$  (Eq. 8). To evaluate the effectiveness of this responsive strategy, it was compared to a null strategy where no resources were invested and  $\Delta r^{opt}(x)$  was set to zero, and a constitutive investment strategy where the resource density is raised uniformly by the maximum  $\Delta r^{opt}(x)$  seen in the responsive strategy (Eq. 9).

### Agent-based model

The agent based model is a program that is based on the Java biofilm model previously published by Xavier *et al.*<sup>6</sup>. The biofilm modelling framework was available as a compiled library of Java classes, which caused version control problems that arose when trying to reproduce the model and results published by Carmona-Fontaine *et al.* The biofilm framework was written to allow the simulation of biofilm microbial species without constraints on the number of solute species, meaning that it integrates detached and structured biomass. If the older version of this biofilm framework required to run the model by Carmona-Fontaine *et al.* was available, it would be more than sufficient to reproduce the agent-based simulation results included in the publication. However, without access to the older version and lacking most of the original parameters used, we were able to reproduce very few of the original results.

### CompuCell3D

Due to the complications experienced with the agent-based model, we attempted to use an alternative modeling system to reproduce the original results. CompuCell3D<sup>7</sup> is a program in XML and Python that was designed for the simulation of populations of cells. It focuses much of its computational effort on the complex physical forces that neighboring cells exert on one another, making simulations of tens of thousands of cells impractical. However, extensive documentation exists for this program, and we were able to customize cell growth rates, diffusion, and communication between cells and vessels according to the equations given by Carmona-Fontaine *et al.*

## Results

### Theoretical Model

The theoretical model described by Carmona-Fontaine *et al.* could be readily reproduced solely via the contents of the paper's Supplementary Information. The values of certain constants used in their model, specifically the cost function weight and the growth rate half-saturation constant, were not given; however, these are likely to vary in a biological system and are often determined empirically. The reproduced responsive, constitutive, and null models behaved identically to those shown in the original paper (Fig. 1). The responsive model mimicked the behavior of the null model and did not secrete VEGF at high resource densities; however, it began investing in VEGF secretion at increasing levels after a certain distance from the resource source was reached.

### Agent-based Model

We were only able to replicate a few partial simulations by Carmona-Fontaine *et al.* The agent-based model runs on the biofilm framework which has been updated several times since

the paper was published. The angiogenesis file that was used in the paper does not reflect these changes, and the classes used in this java file were provided in a compiled format, meaning they could not be updated. The source code was not available; therefore, we could not replace the classes in the angiogenesis model that were missing in the updated biofilm framework. Despite these difficulties, we were able to change a few parameters in the biofilm framework to reflect variables present in the agent-based model. We were able to replicate the changes in oxygen and lactate that occur with distance from the vasculature. Additionally, we were able to simulate the tumor growth curves using different proangiogenic strategies (Fig. 2). Missing important spatial feature parameters such as distance from vasculature meant that most of the other graphs we were able to reproduce were essentially meaningless.

### CompuCell3D

The exact details of the CompuCell3D model differed greatly from those of Carmona-Fontaine *et al.*; for example, Carmona-Fontaine *et al.* modelled cells as rigid circles, while CompuCell3D allows cells to be deformed and stretched by the growth of their neighbors. Despite these differences, we were able to replicate most of the patterns that they documented. We found the same pattern of VEGF secretion by responsive cells at increasing distance from a vessel, in both one and two dimensions (Fig. 3). By adjusting the parameter  $k_r$ , we were able to mimic the spectrum of VEGF secretion strategies that the authors explored: cells that do not secrete VEGF ( $k_r = 0.001$ ), cells that only secrete VEGF when resources are lacking ( $k_r = 1.0$ ), and cells that express VEGF constitutively ( $k_r = 1000.0$ ) (Fig. 4). Under some parameter values, we found that growth rate is higher at intermediate values of  $k_r$ , implying a faster tumor growth rate. This was in agreement with the central finding of Carmona-Fontaine *et al.* The computationally intensive nature of CompuCell3D simulations made it impossible for us to simulate the long-term growth of large tumors that Carmona-Fontaine *et al.* explored in some of their figures (Fig. 5).

## Discussion

Our attempt at reproducing the work of Carmona-Fontaine *et al.* was largely successful. The theoretical model equations and results were identically reproduced and showed that the responsive model balanced the cost of secreting VEGF and the benefit of a faster growth rate by switching between the null and constitutive strategies (Fig. 1). Despite difficulties with the agent-based model, we were able to reproduce some biomass simulations and the concentrations of oxygen and lactate (Fig. 2). Using CompuCell3D, we modeled VEGF secretion within a simulated tumor and measured its effect on growth (Figs. 3-4); however, we were still unable to model tumor biomass over time or compare growth under the constitutive strategy to the responsive strategy (Fig. 5). While the technical difficulties we encountered certainly do not contradict the results presented by Carmona-Fontaine *et al.*, they highlight the difficulties associated with bioinformatics research reproducibility and the importance of version control.

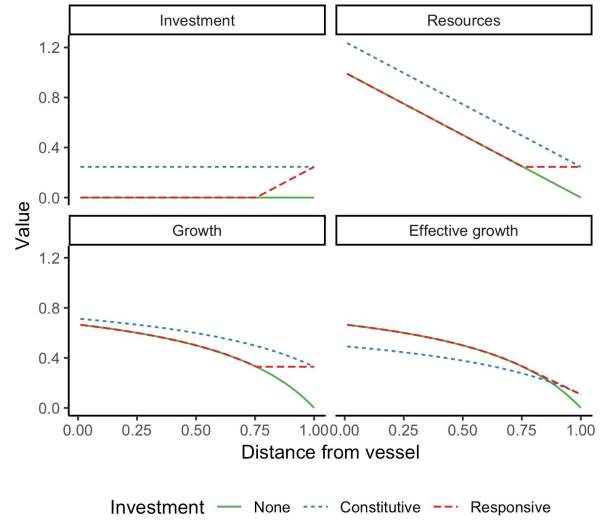
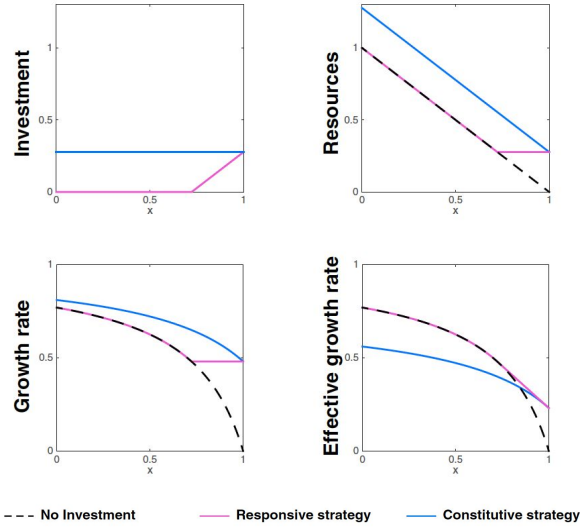
## References

1. Carmona-Fontaine, C., Deforet, M., Akkari, L., *et al.* **“Metabolic Origins of Spatial Organization in the Tumor Microenvironment.”** *Proceedings of the National Academy of Sciences of the United States of America* 114, no. 11 (2017): 2934–2939.  
doi:10.1073/pnas.1700600114
2. Ferrara, N., Gerber, H.-P., and LeCouter, J. **“The Biology of VEGF and Its Receptors.”** *Nature Medicine* 9, no. 6 (2003): 669–676. doi:10.1038/nm0603-669
3. Bates, D. O. **“Vascular Endothelial Growth Factors and Vascular Permeability”** *Cardiovascular Research* 87, no. 2 (2010): 262–271. doi:10.1093/cvr/cvq105
4. Costache, M.I., Ioana, M., Iordache, S., Ene, D., Costache, C. A., and Săftoiu, A. **“VEGF Expression in Pancreatic Cancer and Other Malignancies: A Review of the Literature”** *Romanian Journal of Internal Medicine* 53, no. 3 (2015): 199–208.  
doi:10.1515/rjim-2015-0027
5. Shi, Q., Le, X., Abbruzzese, J. L., Peng, Z., Qian, C.-N., Tang, H., Xiong, Q., Wang, B., Li, X.-C., and Xie, K. **“Constitutive Sp1 Activity Is Essential for Differential Constitutive Expression of Vascular Endothelial Growth Factor in Human Pancreatic Adenocarcinoma”** *Cancer Research* 61, no. 10 (2001): 4143–4154
6. Xavier, J. B., Picioreanu, C., and Loosdrecht, M. C. M. van. **“A Framework for Multidimensional Modelling of Activity and Structure of Multispecies Biofilms”** *Environmental Microbiology* 7, no. 8 (2005): 1085–1103.  
doi:10.1111/j.1462-2920.2005.00787.x
7. Swat, M. H., Thomas, G. L., Belmonte, J. M., Shirinifard, A., Hmeljak, D., and Glazier, J. A. **“Multi-Scale Modeling of Tissues Using CompuCell3D.”** *Methods in Cell Biology* 110, (2012): 325–366. doi:10.1016/B978-0-12-388403-9.00013-8

# Appendix

## Figures

a)



b)

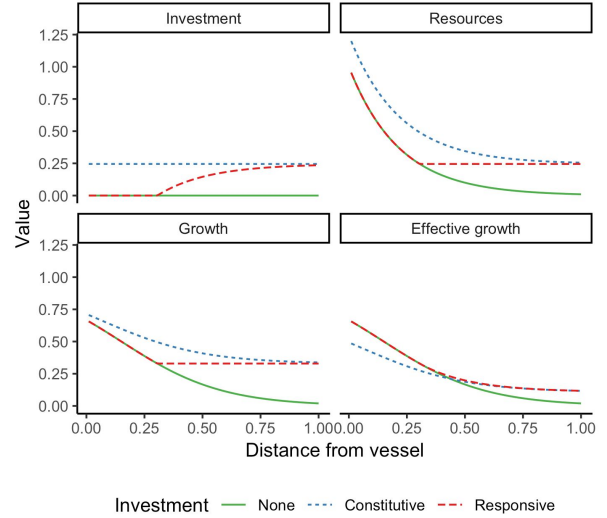
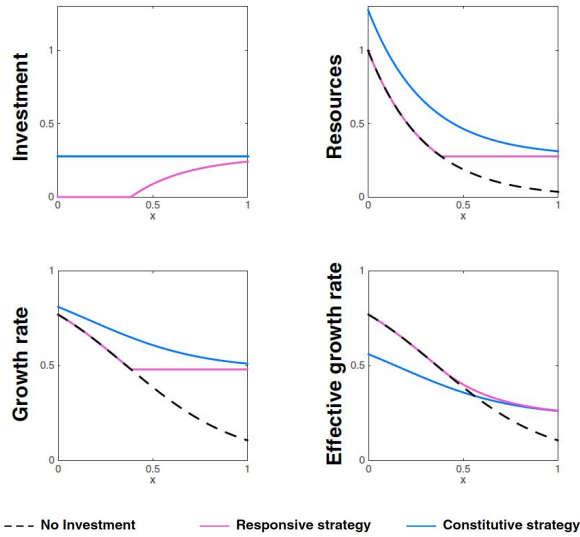
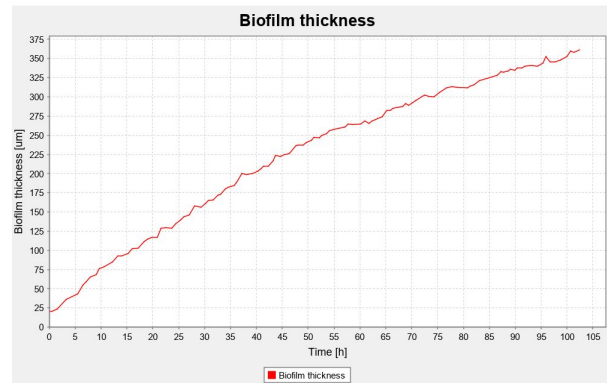
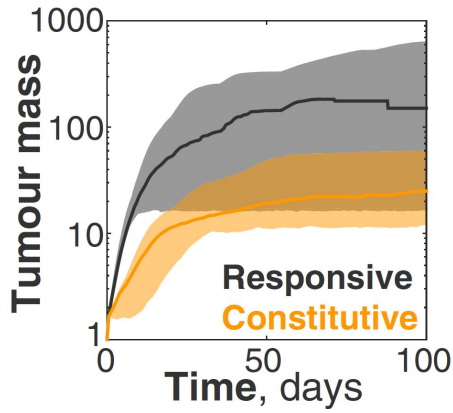
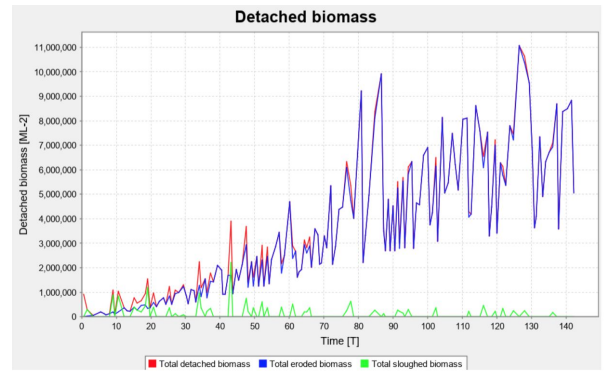
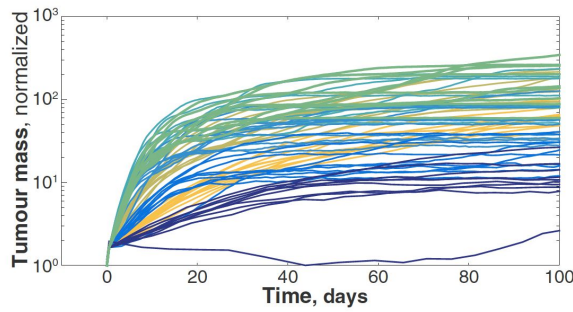


**Figure 1.** The theoretical model could be exactly reproduced using the paper's Supplementary Information. Original figures are on the left, and reproductions are on the right. (a) Linear resource gradient. (b) Exponential resource gradient.

a)



b)



c)

Agent-based simulations

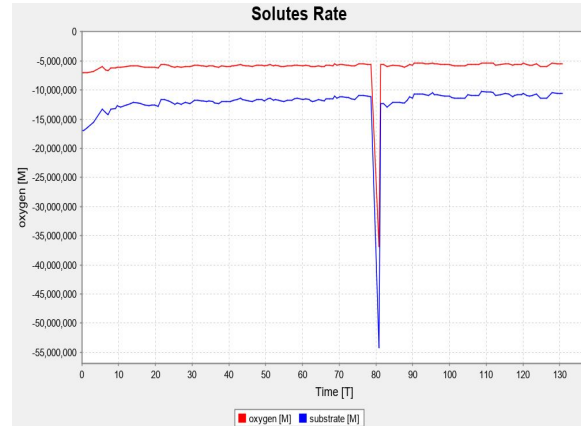
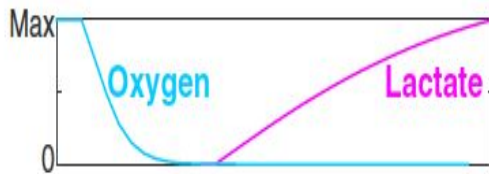


**Figure 2.** The agent-based model was unable to completely reproduce any plots. Original figures are on the left, and partial reproductions are on the right. Original figures are on the order of days, while reproductions were on the order of hours due to computation power constraints. (a) A comparison of responsive and constitutive strategies was attempted using biofilm thickness as an approximation of tumor mass; however, only the responsive strategy could be modeled. (b) Multiple responsive growth simulations as a function of detached biomass could not reproduce the patterns seen in the original paper. (c) Gradients of oxygen and lactate without showing their effect on VEGF as depicted in the paper.

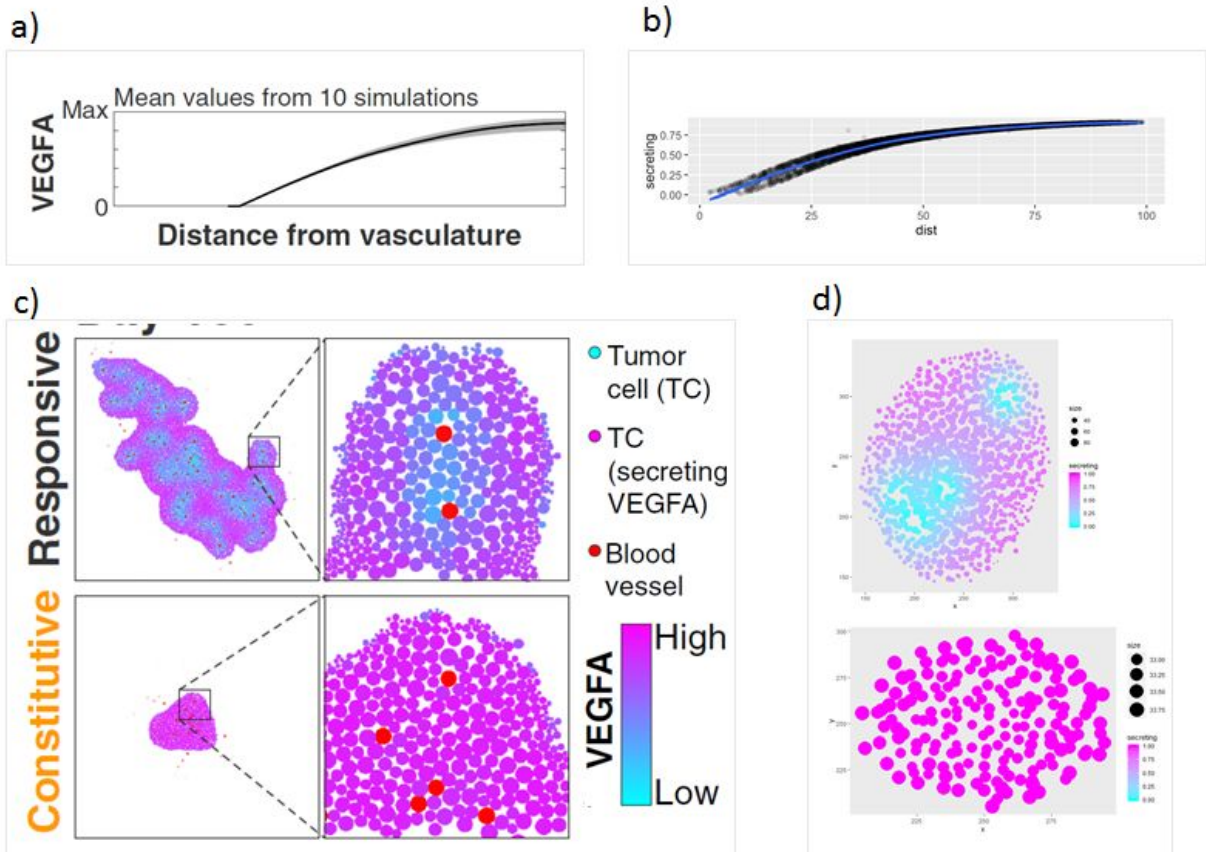


**Figure 3.** Gradient in VEGF secretion with increasing distance from a vessel as reported by Carmona-Fontaine *et al.* (a,c) and the corresponding results from the CompuCell3D model (b,d).

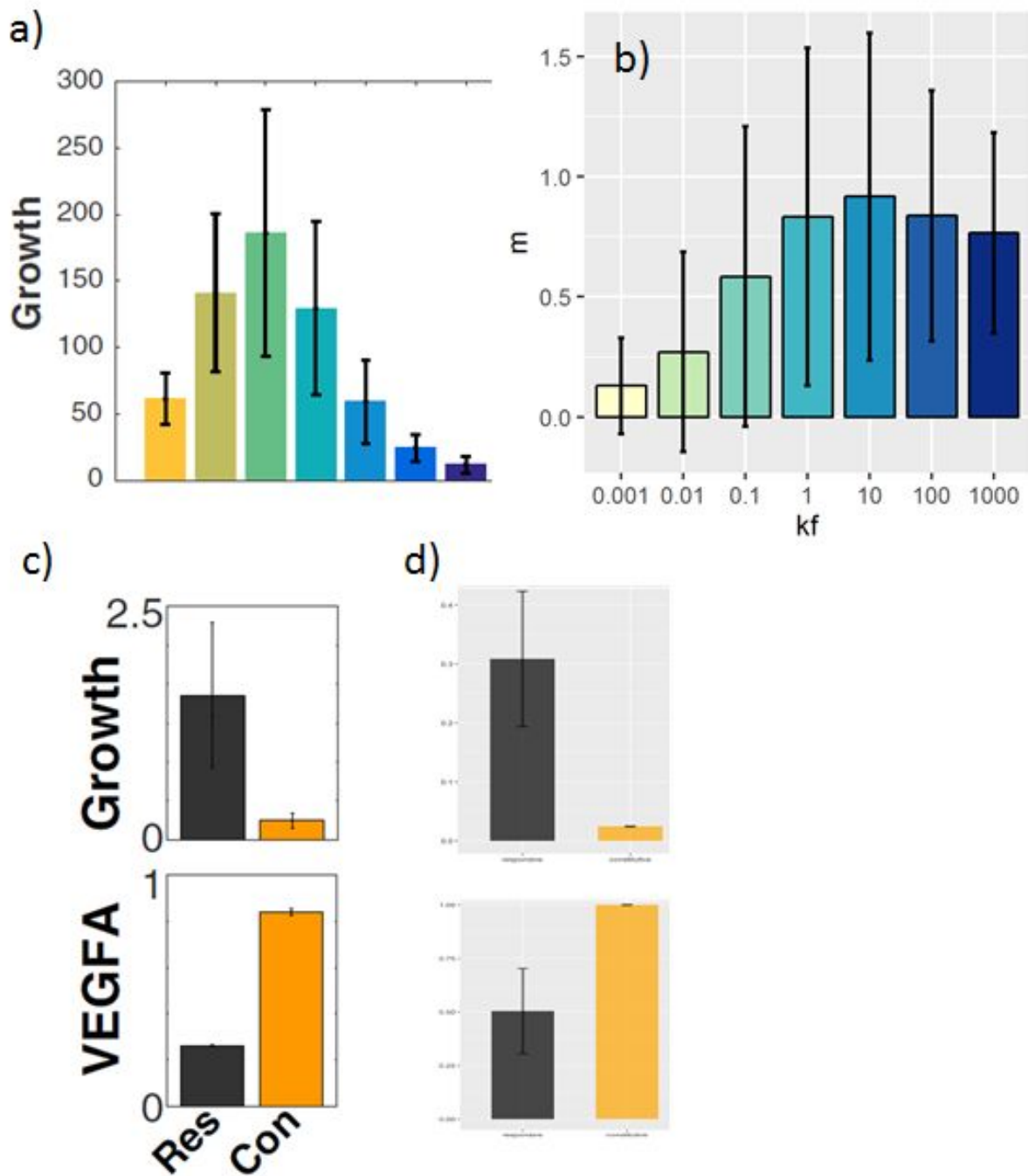


**Figure 4.** Growth rate of simulated cells peaks at intermediate values of  $k_f$  in the responsive strategy as reported by Carmona-Fontaine *et al.* (a, c), and replicated with CompuCell3D (b,d).



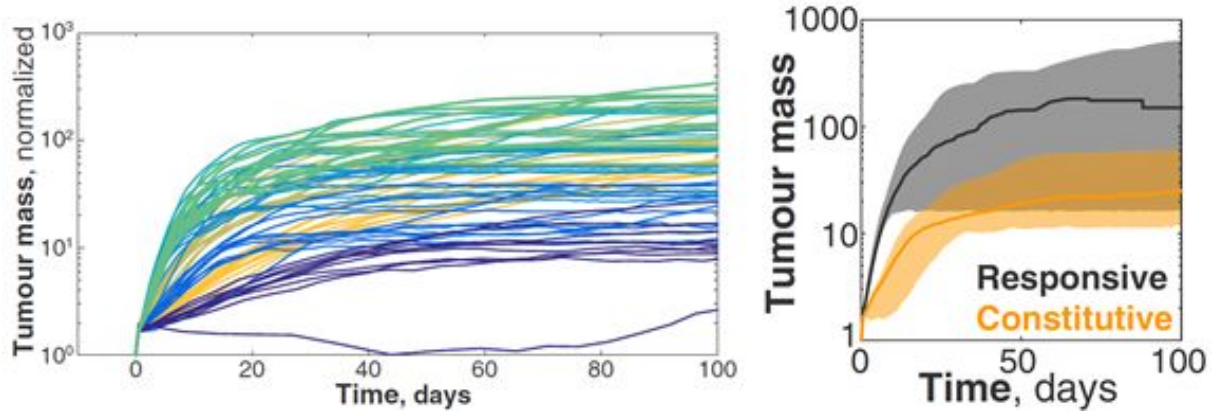


**Figure 5.** Growth curves of simulated tumors as reported by Carmona-Fontaine et al. (2017). Due to computational constraints, we were unable to simulate groups of cells this large with CompuCell3D.

## Equations

**Equation 1.** Linear resource density

$$r(x) = r_{max} \frac{L-x}{L}$$

**Equation 2.** Exponential resource density

$$r(x) = r_{max} b^x$$

**Equation 3.** Cost of increasing resources

$$C(\Delta r) = c\Delta r$$

**Equation 4.** Growth rate follows saturating kinetics

$$\mu(r) = \mu_{max} \frac{r}{r+k}$$

**Equation 5.** Optimal resource density

$$r^{opt} = r(x) + \Delta r^{opt}$$

**Equation 6.** Profit from increasing resource density

$$P(r, \Delta r) = \mu(r(x) + \Delta r) - \mu(r(x)) - c\Delta r$$

**Equation 7.** Optimal growth rate has slope  $c$

$$\begin{aligned}\frac{\delta}{\delta \Delta r} P(r, \Delta r) &= 0 \\ \frac{\delta}{\delta \Delta r} \mu(r(x) + \Delta r) - \frac{\delta}{\delta \Delta r} \mu(r(x)) - \frac{\delta}{\delta \Delta r} c \Delta r &= 0 \\ \frac{\delta}{\delta \Delta r} \mu(r(x) + \Delta r) - c &= 0 \\ \frac{\delta}{\delta \Delta r} \mu(r(x) + \Delta r) &= c\end{aligned}$$

**Equation 8.** Analytical solution to  $\Delta r^{opt}(x)$

$$\begin{aligned}\frac{\delta}{\delta \Delta r} \mu(r(x) + \Delta r) &= c \\ \frac{\delta}{\delta \Delta r} \left( \mu_{max} \frac{r(x) + \Delta r}{r(x) + \Delta r + k} \right) &= c \\ \frac{\mu_{max} k}{(r(x) + \Delta r + k)^2} &= c \\ \sqrt{\frac{\mu_{max} k}{c}} &= r(x) + \Delta r + k \\ \sqrt{\frac{\mu_{max} k}{c}} - k - r(x) &= \Delta r\end{aligned}$$

**Equation 9.**  $\Delta r^{opt}(x)$  for each strategy

$$\text{Null } \Delta r^{opt} = 0$$

$$\text{Constitutive: } \Delta r^{opt} = \sqrt{\frac{\mu_{max} k}{c}} - k$$

$$\text{Responsive: } \Delta r^{opt} = \sqrt{\frac{\mu_{max} k}{c}} - k - r(x)$$

## Author Contributions

Garima Lohani and Caroline Muriithi performed the agent-based modeling. Brian Spitzer implemented the CompuCell3D alternative model. Jacquelyn Turcinovic reproduced the theoretical model results. All authors worked collaboratively to combine the results in the final presentation and report.